Quasicrystalline Al–Cu–Fe and Al–Cu–Co alloys for corrosion-resistant protective coatings

O V Sukhova[1,3] and V A Polonskyy[2]

[1] Chair of Experimental Physics, Oles Honchar Dnipro National University, 72 Gagarin ave., Dnipro 49010, Ukraine
[2] Chair of Physical, Organic and Non-organic Chemistry, Oles Honchar Dnipro National University, 72 Gagarin ave., Dnipro 49010, Ukraine

[3] Corresponding author e-mail: sukhovaya@ukr.net

Abstract. In this work the structure and corrosion behavior of quasicrystalline cast $Al_{63}Cu_{25}Fe_{12}$ and $Al_{63}Co_{24}Cu_{13}$ alloys in 5-% sodium chloride solution (pH 6.9–7.1) were investigated. The alloys were cooled at 5 K/s. The structure of the samples was studied by methods of quantitative metallography, X-ray analysis, and scanning electron microscopy. Corrosion properties were determined by potentiodynamic method. The made investigations confirm the formation of stable quasicrystalline icosahedral (i) and decagonal (D) phases in the structure of $Al_{63}Cu_{25}Fe_{12}$ and $Al_{63}Co_{24}Cu_{13}$ alloys correspondingly. In 5-% sodium chloride solution, the investigated alloys corrode under electrochemical mechanisms with oxygen depolarization. Compared with $Al_{63}Cu_{25}Fe_{12}$ alloy, the value of free corrosion potential for $Al_{63}Co_{24}Cu_{13}$ alloy changes in the positive direction (–0.66 V and –0.43 V, respectively), and its electrochemical passivity region extends due to the inhibition of anodic processes. A corrosion current density, calculated from (E,lg(*i*))-curve, for $Al_{63}Co_{24}Cu_{13}$ alloy amounts to 0.18 mA/cm^2 and for $Al_{63}Cu_{25}Fe_{12}$ alloy – to 0.20 mA/cm^2. The lower corrosion resistance of $Al_{63}Cu_{25}Fe_{12}$ alloy may be explained by the presence of iron-containing phases in its structure. Based on obtained results, the $Al_{63}Co_{24}Cu_{13}$ alloy was recommended as coating material for rocket-and-space equipment working in marine climate.

1. Introduction

The Al–Cu–Fe and Al–Cu–Co alloy systems containing stable quasicrystalline phases are the most interesting functional materials. The interest also is prompted due to the finding of quasicrystalline phases of the above alloys when they are cast under conventional solidification techniques. Three-dimensional Al–Cu–Fe quasicrystals show a five-fold symmetry and have icosahedral structure (i-phase) [1-3]. The Al–Cu–Co quasicrystals are two-dimensional decagonal quasicrystals (D-phase) consisting of periodic stacking of atomic layers with a tenfold symmetry within the plane [4, 5]. Thus, decagonal quasicrystals combine two types of crystalline order: they are quasiperiodic in a plane and they are periodic in the direction perpendicular to a plane. This property sets decagonal phases apart from periodic crystals, as well as from icosahedral quasicrystals.

Quasicrystalline Al–Cu–Fe and Al–Cu–Co alloys may be used as structural components in rocket-and-space industry owing to their high hardness, low surface energy, high wear resistance, low friction, and resistance to oxidation [6–14]. But the quasicrystalline alloys cannot be applied as

functional materials due to their brittle nature at ambient temperature. However, the combination of excellent physical and mechanical properties makes them the promising material for surface application as thick composite [15–18] and ion-plasma thin coatings [19–24] when good corrosion resistance is additionally required.

The rocket-and-space equipment has been currently operating in marine climate, e.g. equipment of mobile platforms for equatorial launches of loads on specialized Zenit-3SL rockets, where salt may affect component surface. Therefore, it is interesting to compare the resistance to corrosion as well as the electrochemical behavior of quasicrystalline cast icosahedral Al–Cu–Fe and decagonal Al–Cu–Co alloys in sodium chloride aqueous solution.

2. Materials and methods

$Al_{63}Cu_{25}Fe_{12}$ and $Al_{63}Co_{24}Cu_{13}$ alloys were prepared of high purity (99.99 %) components put in a graphite crucible and melted using *Tamman* furnace. The cooling rate of the alloys was 5 K/s. In order to verify the bulk compositions, *Sprut SEF-01-M* atomic absorption spectroscopy instrument was applied for the examination of selected samples. The relative precision of the measurements was better than ± 1 at. %.

The instruments used in the microstructural characterization of the investigated alloys were mainly *Neophot* and *GX-51* optical microscopes (OM), *Epiquant* quantitative analyzer, *REMA 102-02* scanning electron microscope (SEM). The alloys were also studied by powder X-ray diffraction (XRD) using *DRON-UM-1* diffractometer with CuK_α radiation. Vickers hardness measurements were carried out at indentation load of 50 g. The data shown was an average of at least 5 measurements.

Electrochemical experiments were conducted in 5-% aqueous sodium chloride solution (pH=6.9–7.1) by means of *PI–50–1* potentiostat and *PR–8* programmer using three-electrode electrolytic system consisted of silver chloride as reference electrode, a platinum as counter electrode, and the sample as working electrode. Potentiodynamic measurements were carried out by sweeping the potential in the positive or negative direction with a sweep rate of 1 mV/s until a current limit in the mA range was reached.

Model corrosion tests for 1, 2, 3, 4, 8 days in a 5-% NaCl solution were performed with specimens 3.0×0.5×0.2 cm in size. The specimens were fully immersed in the saline solution. The surface morphology was examined using a scanning electron microscope (SEM). Corrosion and electrochemical tests were carried out at the temperature of 293±2 K.

3. Results and discussion

The $Al_{63}Cu_{25}Fe_{12}$ alloy exhibits multiphase microstructure (Figure 1, a) [2]. The primary λ-$Al_{13}Fe_4$ phase is nucleated directly from the melt and grows into the liquid, and the β-AlFe(Cu) phase is formed directly from the liquid or via a peritectic reaction between the primary λ and liquid. The λ-phase is surrounded by a shell of the quasicrystalline icosahedral i-Al_6Cu_2Fe phase that is formed afterward via peritectic reaction. The peritectic reaction does not go to completion and the remaining liquid solidifies into low-temperature metastable crystalline phases such as τ-AlCu(Fe), η-AlCu, and θ-Al_2Cu. The i and λ phases are dominant. Their volume fraction measured by quantitative metallography amounts to 55.5 and 32.0 vol. % respectively.

Examination by light-optical microscopy reveals that $Al_{63}Co_{24}Cu_{13}$ alloy consists of three phases identified as quasicrystalline decagonal D-phase, crystalline $Al_4(Co,Cu)_3$ phase, crystalline $Al_3(Cu,Co)_2$ phase (Figure 1, b) [4]. After etching grey-colored quasicrystalline D-phase takes about 65 % of a total alloy volume. The solidification of the D-phase proceeds as a peritectic reaction, in which the primary $Al_4(Co,Cu)_3$ phase is surrounded by the D-phase. Subsequently $Al_3(Cu,Co)_2$ phase solidifies thus producing a three-phase peritectic structure.

Corrosion behavior of the icosahedral and decagonal quasicrystalline phases in the $Al_{63}Cu_{25}Fe_{12}$ and $Al_{63}Co_{24}Cu_{13}$ alloys is tested in 5-% NaCl solution which allows a comparison of their corrosion resistance under conditions comparable to application. Model immersion tests show that corrosion resistance of the $Al_{63}Cu_{25}Fe_{12}$ alloy is noticeably inferior to that of the $Al_{63}Co_{24}Cu_{13}$ alloy (Table 1). In

a daytime, the surface of the $Al_{63}Cu_{25}Fe_{12}$ alloy loses its metallic luster, and gas bubbles appear here. Specific mass change (Δm) reaches 0.81 mg/cm^2.

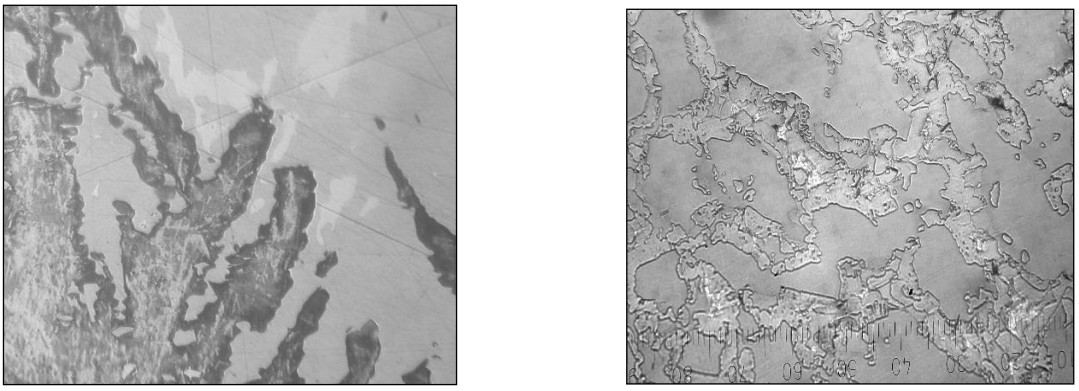

a b

Figure 1. OM images of the investigated alloys (x400): a – $Al_{63}Cu_{25}Fe_{12}$; b – $Al_{63}Co_{24}Cu_{13}$

In a three-day time, the numerous corrosion damages and intensive gas evolution are observed on the surface. Corrosion products go partially into the solution and, therefore, the solution loses transparency. Eight days later, corrosion intensifies (Δm=2.28 mg/cm^2). During the experiments, the pH of the working solution gradually increases which indicates that the sample corrodes under electrochemical mechanism with oxygen depolarization and formation of OH^- ions. Most likely, at the initial stage of corrosion, the surface iron atoms may be oxidized and act as anodes in galvanic couple. In contact with water and oxygen, the Fe^{2+} ions turn into Fe^{3+} ions. Final corrosion product observed visually on the surface is $xFe_2O_3 \cdot yH_2O$ compound of non-stochiometric composition (brown rust). This layer formation is consistent with the change in color of the samples seen during the immersion.

Table 1. The specific mass change (in mg/cm^2) of $Al_{63}Cu_{25}Fe_{12}$ and $Al_{63}Co_{24}Cu_{13}$ alloys affected by 5-% NaCl solution.

Alloy	Holding time, days				
	1	2	3	4	8
$Al_{63}Cu_{25}Fe_{12}$	0.81	1.39	1.47	2.28	2.74
$Al_{63}Co_{24}Cu_{13}$	0.12	0.48	0.65	0.72	0.80

The substitution of iron and copper by cobalt in Al–Cu–Fe alloy is favorable for the essential increase of the corrosion resistance of the samples. After 8 days of the tests, the mass change of the $Al_{63}Co_{24}Cu_{13}$ alloy equals to 0.80 mg/cm^2 (Table 1). Only single gas bubbles are observed on the surface; color and transparency of working solution do not practically change. Gradual inhibition of a corrosion rate of the cobalt-containing alloy indicates that a passivation film consisted of corrosion products is formed during the tests. This film may be revealed visually as surface darkening that shows no color change of the surface with immersion duration. So, for the $Al_{63}Co_{24}Cu_{13}$ alloy, behavior is consistent with the formation of a passive layer.

The results of model immersion tests are in good agreement with chronopotentiometry measurements of free corrosion potentials (E) of the $Al_{63}Cu_{25}Fe_{12}$ and $Al_{63}Co_{24}Cu_{13}$ alloys in 5-% neutral NaCl solution. Figure 2 shows that for $Al_{63}Cu_{25}Fe_{12}$ alloy the potential stabilizes at the value of –0.66 V during more than 7,000 seconds (2 hours).

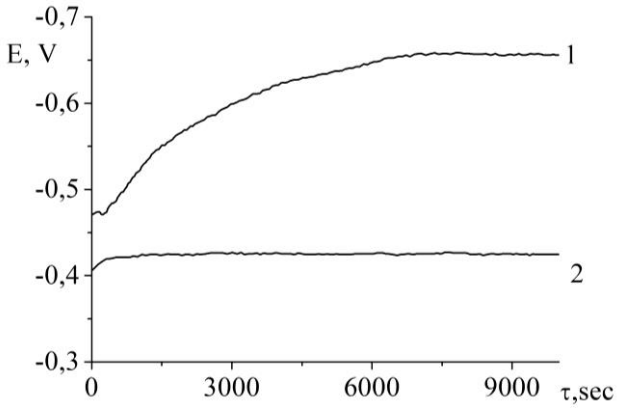

Figure 2. (E,τ)-curves recorded for $Al_{63}Cu_{25}Fe_{12}$ (1) and $Al_{63}Co_{24}Cu_{13}$ (2) alloys in 5-% NaCl solution (pH=7.0).

For $Al_{63}Co_{24}Cu_{13}$ alloy, a potential has value (–0.43 V) that stops changing no longer than after 1,000 seconds of measurements. A change of potential in the positive direction indicates the formation of a passive film and a steady potential indicates that the film remains intact and protective. So, as evidenced by obtained results, $Al_{63}Co_{24}Cu_{13}$ alloy is more corrosion resistant due to surface passivation.

In Figure 3 are shown voltammograms recorded at potentials in the anodic direction from the stationary value up to a sharp increase of a current density due to oxidation of the alloys' constituents. After changing the direction of a potential sweep, in the cathodic area of a plot, the region of corrosion current limit is observed that is typical to corrosion processes with oxygen depolarization. At the reverse cycle of a potential sweep, the electrochemical passivity region may be determined. For $Al_{63}Cu_{25}Fe_{12}$ alloy this region extends from –1.0 V to –0.6 V, and for $Al_{63}Co_{24}Cu_{13}$ alloy from –1.0 V to –0.4 V. The extension of the passivity region towards more positive potentials indicates that the $Al_{63}Co_{24}Cu_{13}$ alloy is less susceptible to corrosion than the $Al_{63}Cu_{25}Fe_{12}$ alloy.

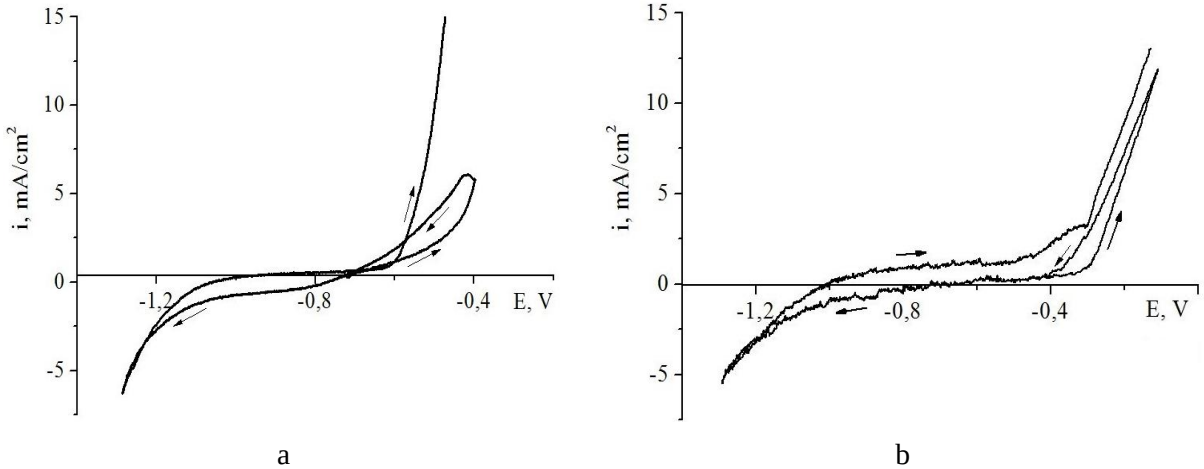

Figure 3. Cyclic voltammograms recorded in 5-% NaCl solution (pH=7.0) for: a – $Al_{63}Cu_{25}Fe_{12}$; b – $Al_{63}Co_{24}Cu_{13}$ alloys

Figure 4 shows the results of voltammetry presented in semi-logarithmic coordinates in order to determine corrosion current density (i). The intersection point of two plot branches corresponds to a logarithm of i. The value of corrosion current density determined for the $Al_{63}Cu_{25}Fe_{12}$ alloy equals to 0.20 mA/cm^2 (Figure 4, a), and that for the $Al_{63}Co_{24}Cu_{13}$ alloy is 0.18 mA/cm^2 (Figure 4, b) which may relate to the inhibition of anodic processes for the $Al_{63}Co_{24}Cu_{13}$ alloy.

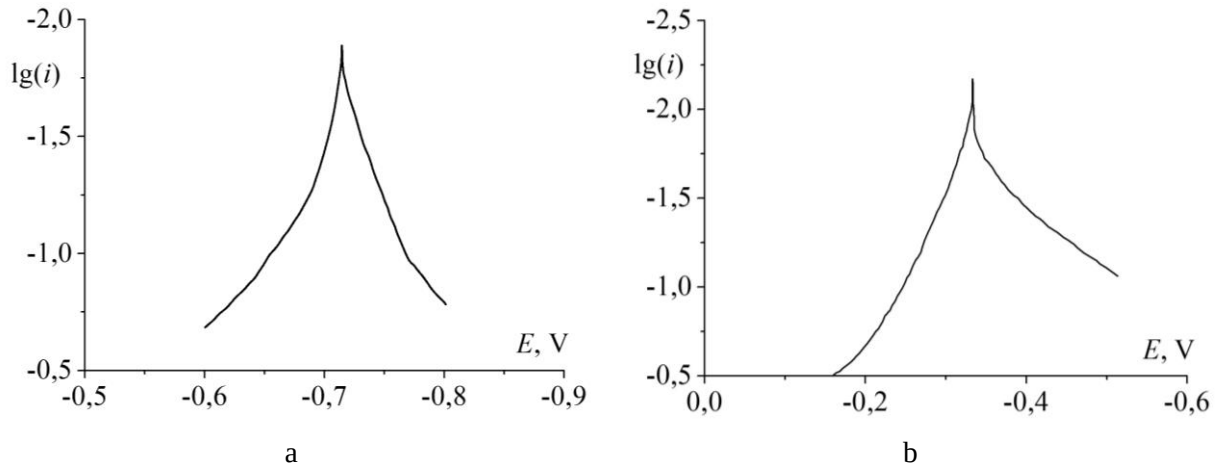

a b

Figure 4. (E,lg(*i*))-curves recorded in 5-% NaCl solution (pH=7.0) for: a – $Al_{63}Cu_{25}Fe_{12}$; b – $Al_{63}Co_{24}Cu_{13}$ alloys

The SEM images of the surface of the $Al_{63}Cu_{25}Fe_{12}$ alloy corroded in 5-% sodium chloride solution evidence that after the 8-day tests pits are observed on the surface of the alloy (Figure 5, a). Pits sites, sized from 10 to 50 μm, are non-uniformly distributed on the surface. Corrosion occurs primarily in the iron-rich λ-phase and secondarily in the quasicrystalline i-phase. The pits bottom is commonly covered by a porous layer of undissolved copper. The remains of non-separated brown rust are revealed on the alloy surface as well.

On the surface of $Al_{63}Co_{24}Cu_{13}$ alloy, pits about 10 μm in size located mainly in the vicinity of defects are also revealed (Figure 5, b). In addition to pitting, the boundaries between the primary and peritectic phases are preferentially dissolved.

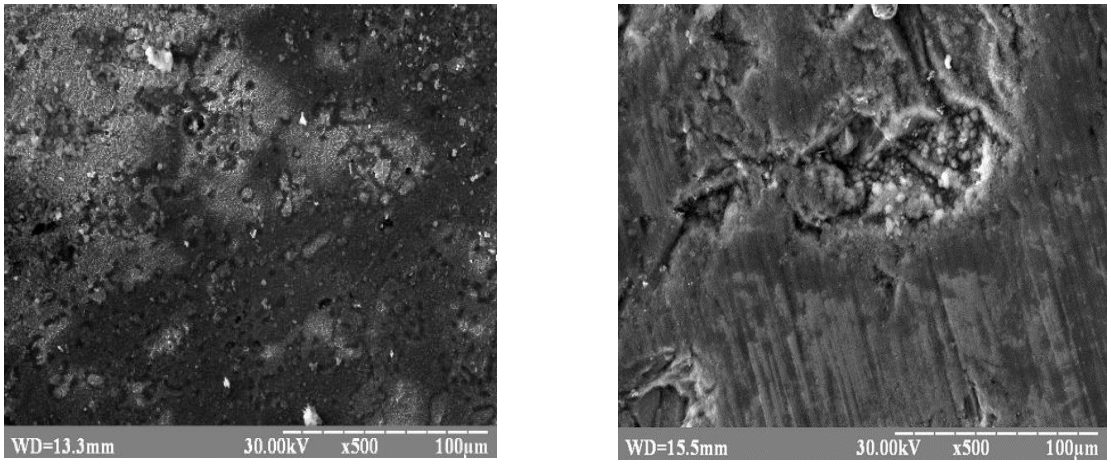

a b

Figure 5. SEM-images of the surface of the alloys after 8-day immersion test in 5-% NaCl solution (pH=7.0): a – $Al_{63}Cu_{25}Fe_{12}$; b – $Al_{63}Co_{24}Cu_{13}$

Thus, from the electrochemical point of view, the $Al_{63}Cu_{25}Fe_{12}$ and $Al_{63}Co_{24}Cu_{13}$ alloys behave quite similarly in the aqueous sodium chloride solution, but immersion tests show that on the surface of $Al_{63}Cu_{25}Fe_{12}$ alloy larger pits appear in greater quantity. So, a first order assessment would suggest that the $Al_{63}Cu_{25}Fe_{12}$ alloy has lower resistance to pitting than the $Al_{63}Co_{24}Cu_{13}$ alloy. The reason is that iron-rich phases and their boundaries in the structure of the $Al_{63}Cu_{25}Fe_{12}$ alloy are more susceptible to attack by saline solution. The pits on the surface of the $Al_{63}Cu_{25}Fe_{12}$ alloy are Cu-rich, apparently forming by dissolution of Fe and Al, and those on the surface of the $Al_{63}Co_{24}Cu_{13}$ alloy are

Co- and Cu-rich due to preferential dissolution of Al. Hence, the general trend seems to be that the noblest metals remain at the surface during corrosion, while the other components, such as Fe and/or Al, dissolve. Corrosion is controlled mainly by chemical composition of the investigated alloys rather than the specific atomic structure of icosahedral or decagonal quasicrystalline phases present in their structure.

Conclusions

The investigations performed on conventionally solidified $Al_{63}Cu_{25}Fe_{12}$ and $Al_{63}Co_{24}Cu_{13}$ alloys confirm that both alloy systems cooled at 5 K/s form stable quasicrystalline icosahedral (i) and decagonal (D) phases correspondingly. In $Al_{63}Cu_{25}Fe_{12}$ alloy, the primarily solidified phase is λ-$Al_{13}Fe_4$ but, in $Al_{63}Co_{24}Cu_{13}$ alloy, the $Al_4(Co,Cu)_3$. Quasicrystalline i and D phases are further formed by peritectic reaction.

The corrosion of the investigated alloys in 5-% NaCl aqueous solution (pH 6.9–7.1) occurs by the electrochemical mechanism with oxygen depolarization. More electropositive copper acts as cathode and more electronegative iron or cobalt – as anode.

When subjected to corrosion, iron-rich phases (λ та i) of $Al_{63}Cu_{25}Fe_{12}$ alloy selectively oxidize, with water soluble Fe^{2+} compounds forming. Affected by oxygen and water, these compounds turn into insoluble Fe^{3+} compounds that accumulate on the surface of the alloy and may partially separate from it.

As compared with $Al_{63}Cu_{25}Fe_{12}$ alloy, $Al_{63}Co_{24}Cu_{13}$ alloy shows better corrosion resistance which may relate to the formation of passive cobalt-containing compounds blocking the surface. This alloy has less negative free corrosion potential, wider electrochemical passivity region as well as scarcer and smaller pits on the surface affected by saline solution. Therefore, the $Al_{63}Co_{24}Cu_{13}$ alloy shows promise as a coating material to protect rocket-and-space equipment working in marine atmosphere.

References

[1] Faudot F, Quivy A, Calvayrac Y, Gratias D and Harmelin M 1991 About the Al-Cu-Fe icosahedral phase formation *Materials Science and Engineering* **Volume A133** pp 383-387 https://doi.org/10.1016/0921-5093(91)90093-3

[2] Huttunen-Saarivirta E 2004 Microstructure, fabrication and properties of quasicrystalline Al–Cu–Fe alloys: a review *Journal of Alloys and Compounds* **Volume 363(1-2)** pp 150-174 https://doi.org/10.1016/S0925-8388(03)00445-6

[3] Sukhova O V and Ustinova K V 2019 The effect of cooling rate on phase composition of quasicrystalline Al-Cu-Fe alloys doped with Si and B *Functional Materials* **Volume 26(3)** pp 495-506 https://doi.org/10.15407/fm26.03.495

[4] Tsai A P, Inoue A and Masumoto T 1989 A stable decagonal quasicrystal in the Al-Cu-Co system *Materials Transactions JIM* **Volume 30(4)** pp 300-304 https://doi.org/10.2320/matertrans1989.30.300

[5] Grushko B 1992 The composition of the decagonal quasicrystalline phase in the Al–Cu–Co alloy system *Phylosophical Magazine Letters* **Volume 66(3)** pp 151-157 https://doi.org/10.1080/09500839208229278

[6] Kang S S and Dubois J M 1993 Tribological properties of quasicrystalline coatings *Journal of Materials Research* **Volume 8(10)** pp 2471-2481 https://doi.org/10.1557/jMR.1993.2471

[7] Rampulla D M, Mancinelli C M, Brunell I F and Gellman A J 2005 Oxidative and tribological properties of amorphous and quasicrystalline approximant Al-Cu-Fe thin films *Langmuir* **Number 6** pp 4547-4553 https://doi.org/10.1021/la0469093

[8] Matthews R P, Lang C I and Shechtman D 1999 Sliding wear of quasicrystalline coatings *Tribology Letters* **Number 7** pp 179-181 https://doi.org/10.1023/A:1019185707264

[9] Rudiger A and Koster U 2000 Corrosion behavior of Al-Cu-Fe quasicrystals *Materials Science and Engineering* **Volume 294-296** pp 890-893 https://doi.org/10.1016/S0921-5093(00)01037-6

[10] Rudiger A and Koster U 1999 Corrosion of Al-Cu-Fe quasicrystals and related crystalline phases *Journal of Non-Crystalline Solids* **Volume 250-252** pp 892-902 https://doi.org/10.1016/S0022-3093(99)00201-X
[11] Huttunen-Saarivirta E and Tiainen T 2004 Corrosion behaviour of Al–Cu–Fe alloys containing a quasicrystalline phase *Materials Chemistry and Physics* **Volume 85(2-3)** pp 383-395 https://doi.org/10.1016/j.matchemphys.2004.01.025
[12] Sukhova O V, Polonskyy V A and Ustinova K V 2019 Corrosion resistance of alloys of the Al-Cu-Fe-(Si, B) system in mineralized saline and acid solutions *Materials Science* **Volume 55(2)** pp 285-292 https://doi.org/10.1007/s11003-019-00302-2
[13] Zhou C, Cai R, Gong S and Xu H 2006 Hot corrosion of AlCuFeCr quasicrystalline coating on titanium alloys with NaCl deposit *Surface Coating Technology* **Volume 201** pp 1718-1723 https://doi.org/10.1016/j.surfcoat.2006.02.043
[14] Kang Y, Zhou C, Gong S and Xu H 2005 Corrosion of Al-Cu-Fe-Cr quasicrystalline coating *Materials Science Forum* **Volume 475-479** pp 3355-3358 https://doi.org/10.4028/www.scientific.net/MSF.475-479.3355
[15] Spiridonova I M , Sukhovaya E V , Pilyaeva S B and Bezrukavaya O G 2002 The use of composite coatings during metallurgical equipment parts repair *Metallurgical and Mining Industry* **Number 3** pp 58-61
[16] Laplanche G, Joulain A and Bonneville J 2010 Microstructures and mechanical properties of Al-base composite materials reinforced by Al–Cu–Fe particles *Journal of Alloys and Compounds* **Volume 493(1-2)** pp 453-460 https://doi.org/10.1016/j.jallcom.2009.12.124.
[17] Sukhova O V, Syrovatko Yu V 2011 Features of structurization of composite materials of the solution-and-diffusion type *Metallofizika i Noveishie Tekhnologii* **Volume 33(Special Issue)** pp 371-378
[18] Spiridonova I M, Sukhova O V and Vashchenko A P 1999 Multicomponent diffusion processes in boride-containing composite materials *Metallofizika i Noveishie Tekhnologii* **Volume 21(2)** pp 122-125
[19] Dubois J M, Kang S S and Massiani Y 1993 Application of quasicrystalline alloys to surface coating of soft metals *Journal of Non-Crystalline Solids* **Volume 153-154** pp 443-445 https://doi.org/10.1016/0022-3093(93)90392-B
[20] Chabak Yu G, Fedun V I, Pastukhova T V, Zurnadzhy V I, Berezhnyy S P and Efremenko V G 2017 Modification of steel surface by pulsed plasma heating *Problems of Atomic Science and Technology* **Volume 110(4)** pp 97-102
[21] Duriagina Z A, Kovbasyuk T M and Bespalov S A 2016 The analysis of competitive methods of improvement of operational properties of functional layers of flat heating elements *Uspekhi Fiziki Metallov* **Volume 17(1)** pp 29-51 https://doi.org/10.15407/ufm.17.01.029
[22] Duryagina Z A, Bespalov S A, Pidkova V Ya and Polockyj D Yu 2011 Examination of the dielectric layers on the structural materials formed by hybrid ion-plasma discharge system *Metallofizika i Noveishie Tekhnologii* **Volume 33(Special Issue)** pp 393-398
[23] Efremenko V G, Chabak Yu G, Lekatou A, Karantzalis A E and Efremenko A V 2016 High-temperature oxidation and decarburization of 14.55 wt pct Cr-cast iron in dry air atmosphere *Metallurgical and Materials Transactions A* **Volume 47(2)** pp 1529-1543 https://doi.org/10.1007/s11661-018-4722-0
[24] Ryabtsev S I, Polonskyy V A and Sukhova O V 2020 Effect of scandium on the structure and corrosion properties of vapor-deposited nanostructural quasicrystalline Al-Cu-Fe films *Powder Metallurgy and Metal Ceramics* **Volume 58(9-10)** pp 567-575 https://doi.org/10.1007/s11106-020-00111-2